In Vivo Hypoxia Monitoring via Magnetic Resonance Imaging for Mouse Models

Needa Virani, PhD[1*], Andrea Protti, PhD[2], Jihun Kwon, PhD[1,3], Heling Zhou, PhD[4], and Ralph Mason, PhD[4], & Ross Berbeco, PhD[1]

[1]Department of Radiation Oncology, Brigham and Women's Hospital, Dana-Farber Cancer Institute, & Harvard Medical School, Boston, MA
[2]Lurie Family Imaging Center, Department of Radiology, Dana-Farber Cancer Institute & Harvard Medical School, Boston, MA
[3]Hokkaido University, Sapporo, Japan
[4]Department of Radiology, The University of Texas Southwestern Medical Center, Dallas, TX

Contact Information
Needa Virani, navirani@bwh.harvard.edu

Introduction

Serial hypoxia measurements have gained interested over the past few years as a means to monitor tumor development and evaluate treatment progression. Current techniques for hypoxia measurements include *ex vivo* biopsies followed by immunohistochemistry, which limits multiple serial measurements, or Positron Emission Tomography, which is limited by low spatial resolution and need for radioactive isotopes. Magnetic Resonance Imaging (MRI) is an alternative approach mitigating the need for contrast agents as well as providing improved resolution.

A functional MRI approach, blood oxygen level dependent (BOLD), uses a gradient echo sequence with an oxygen challenge to monitor changes in T2*,which is affected by the level of deoxyhemoglobin within the blood. In normoxic tissue, it is expected that during a hyperoxic gas challenge T2* values will increase as deoxyhemoglobin is saturated with oxygen; in contrast, in hypoxic tissue, T2* is expected to remain stagnant.

This study applies a BOLD sequence with an in-house MATLAB analysis to an orthotopic murine glioblastoma model. A training cohort was used to optimize post-image analysis parameters comparing MRI slices with their respective pimonidazole immunohistochemistry (IHC) sections. Pearson's correlations were used to identify optimal "thresholding" T2* ranges and ΔT2* values, which were then applied to a validation cohort. A strong Pearson's correlation of 0.781 ($p<0.01$) was identified when comparing the BOLD MRI slices with their respective IHC sections during the validation phase.

This work confirms the use of BOLD MRI on a murine glioblastoma model to identify hypoxic regions using an in-house MATLAB analysis technique that can be reoptimized and applied to other murine models or disease sites.

Data Acquisition

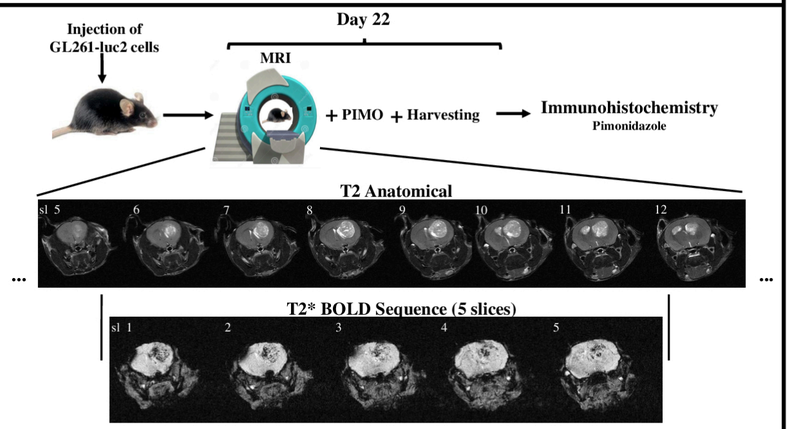

Figure 1: Workflow of data acquisition. MR imaging and immunohistochemistry (IHC) sample collection is depicted. Female B6(Cg)-Tyrc-2J/J mice were orthotopically injected with GL261-luc2 cells. At day 22 post-tumor cell injection, mice underwent BOLD MRI. Initially, anatomical fast spin-echo (FSE) T2-weighted scans were performed to localize the tumor. Within the tumor, 5 slices (0.5 mm thick) were selected for BOLD imaging. A T2*-weighted gradient-echo sequence (GRE) with an oxygen challenge was run over 20 scans (10 air-breathing and 10-oxygen breathing). Following MRI acquisition, mice were injected intravenously with pimonidazole (PIMO) and tissue was collected for immunohistochemistry (IHC) after 90 mins.

Data Analysis

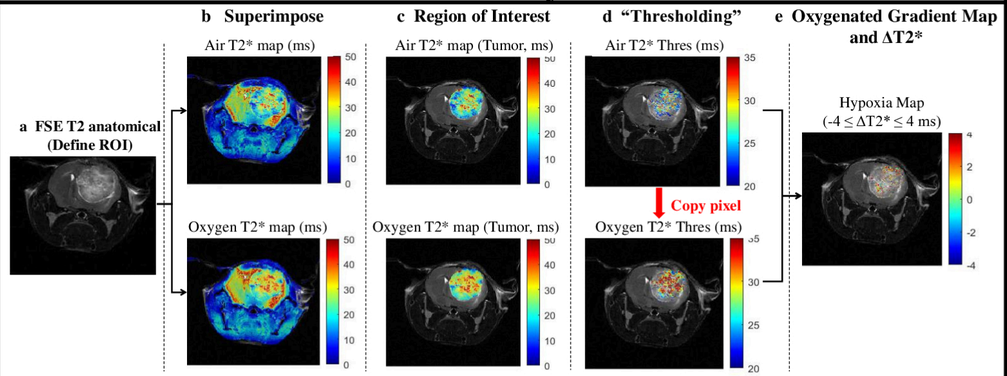

Figure 2: Workflow of MRI image analysis in MATLAB. (a) FSE images were used to identify tumor ROI per slice. **(b)** Superimpose: T2* maps for mice breathing air and oxygen were generated and superimposed on the FSE image. **(c)** Region of interest: Tumor ROI T2* maps were further superimposed on the FSE image to limit the subsequent analysis to the region of interest. **(d)** "Thresholding": Air-breathing T2* maps were thresholded based on values determined during training and the respective pixel mask was applied to the oxygen-breathing T2* map. **(e)** Oxygenated Gradient Map and ΔT2*: Oxygen and air maps were subtracted and areas with low (ΔT2* ≤ ±4ms) change were highlighted as hypoxic.

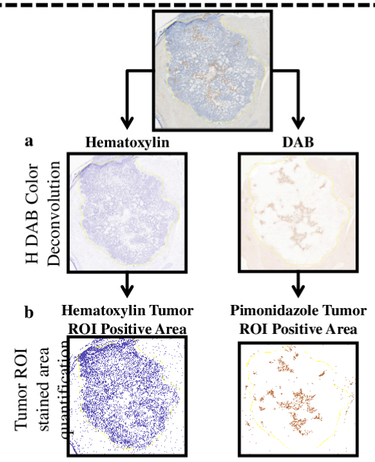

Figure 3: ImageJ pimonidazole IHC analysis workflow. (a) An ImageJ hematoxylin and DAB color deconvolution plugin (H DAB) was utilized to separate cell nuclei positive for hematoxylin (blue) and hypoxia regions positive for pimonidazole (brown). **(b)** Following deconvolution, a region of interest (ROI) was drawn on the original IHC image and was applied to each deconvoluted image followed by positive area quantification. The final percent positive pimonidazole values were derived by comparing the pimonidazole deconvoluted image positively stained area against the hematoxylin positively stained area.

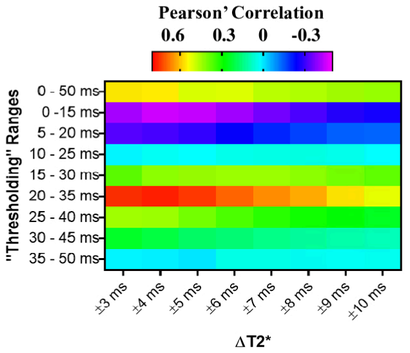

Figure 4: Pearson's correlation of different combinations of T2* "thresholding" ranges and ΔT2* values applied to the T2* maps during the training phase. The optimal hypoxia parameters were identified by comparing the MRI hypoxia positive area per slice with their respective pimonidazole IHC sections. The parameters with the highest correlation ($20 \leq T2^* \leq 35$ ms and $\Delta T2^* = \pm 4$ ms) were applied during the validation phase.

Training Cohort

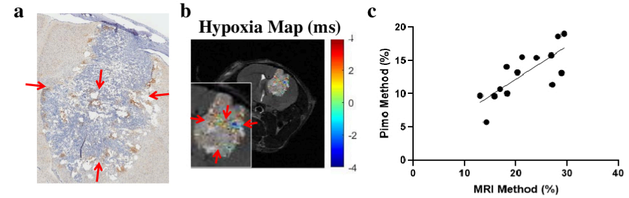

Figure 5: Training cohort correlation between respective MRI slices and pimonidazole sections. Representative **(a)** pimonidazole IHC and **(b)** hypoxia MRI map is shown. Qualitatively, there is similar localization between the areas identified as hypoxic (red arrows) when comparing the MRI maps to the respective pimonidazole IHCs. **(c)** Four to five slices were evaluated for each animal with both MRI and IHC for percent hypoxic region within the tumor. A strong Pearson's correlation (0.767, $p < 0.01$) was identified between MRI positive hypoxia regions versus pimonidazole positive regions.

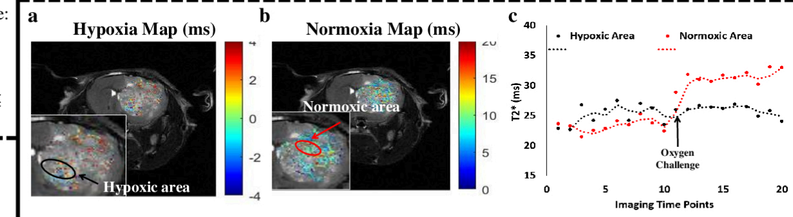

Figure 6: Monitoring dynamic T2* during oxygen challenge. Representative **(a)** hypoxia and **(b)** potential normoxia ΔT2* maps. The region circled in black identifies a hypoxic area with minimal change in T2* values, while the region circled in red shows lengthening in T2*. **(c)** This is also seen when dynamically comparing T2* over time with the addition of an oxygen challenge. The region within the black circle has minimal dynamic change in T2* while the normoxic tissue has a noticeable lengthening in T2* (red circle) following the oxygen challenge.

Validation Cohort

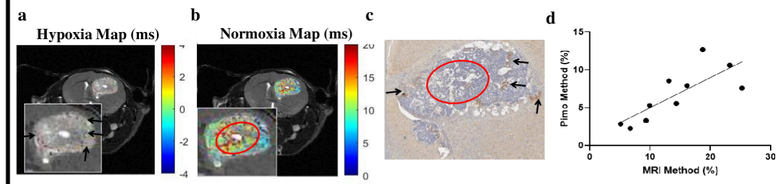

Figure 7: MRI BOLD analysis of validation cohort. A representative **(a)** hypoxia map and **(b)** normoxia map from the validation cohort is shown with black arrows highlighting identified regions of hypoxia and a red circle representing potential normoxic tissue. These MRI images were then compared against their respective pimonidazole sections to prove the validity of the optimized BOLD MRI post-image analysis. **(c)** The pimonidazole section is shown for the same MRI slice confirming similar areas of hypoxia (black arrows) and non-stained tissue, potential normoxia (red circle). **(d)** When comparing the larger validation cohort of MRI images with their respective pimonidazole IHCs, a strong Pearson's correlation (0.781, $p<0.01$) is identified between both methods.